Original Article

Coronary CTA using scout-based automated tube potential and current selection algorithm, with breast displacement results in lower radiation exposure in females compared to males

Harshna Vadvala, Phillip Kim, Thomas Mayrhofer, Oleg Pianykh, Mannudeep Kalra, Udo Hoffmann, Brian Ghoshhajra

Department of Radiology, Massachusetts General Hospital, Harvard Medical School, Boston, MA 02114, USA

Correspondence to: Brian Ghoshhajra, MD, MBA. Assistant Professor of Radiology, Harvard Medical School; Clinical Director, Cardiac CT and MRI Imaging. Cardiac MR PET CT Program, Department of Radiology, Massachusetts General Hospital, Harvard Medical School, 165 Cambridge Street, Suite 400, Boston, MA 02114, USA. Email: bghoshhajra@mgh.harvard.edu.

Purpose: To evaluate the effect of automatic tube potential selection and automatic exposure control combined with female breast displacement during coronary computed tomography angiography (CCTA) on radiation exposure in women versus men of the same body size.

Materials and methods: Consecutive clinical exams between January 2012 and July 2013 at an academic medical center were retrospectively analyzed. All examinations were performed using ECG-gating, automated tube potential, and tube current selection algorithm (APS-AEC) with breast displacement in females. Cohorts were stratified by sex and standard World Health Organization body mass index (BMI) ranges. CT dose index volume ($CTDI_{vol}$), dose length product (DLP) median effective dose (ED), and size specific dose estimate (SSDE) were recorded. Univariable and multivariable regression analyses were performed to evaluate the effect of gender on radiation exposure per BMI.

Results: A total of 726 exams were included, 343 (47%) were females; mean BMI was similar by gender (28.6±6.9 kg/m^2 females *vs.* 29.2±6.3 kg/m^2 males; P=0.168). Median ED was 2.3 mSv (1.4-5.2) for females and 3.6 (2.5-5.9) for males (P<0.001). Females were exposed to less radiation by a difference in median ED of –1.3 mSv, $CTDI_{vol}$ –4.1 mGy, and SSDE –6.8 mGy (all P<0.001). After adjusting for BMI, patient characteristics, and gating mode, females exposure was lower by a median ED of –0.7 mSv, $CTDI_{vol}$ –2.3 mGy, and SSDE –3.15 mGy, respectively (all P<0.01).

Conclusions: We observed a difference in radiation exposure to patients undergoing CCTA with the combined use of AEC-APS and breast displacement in female patients as compared to their BMI-matched male counterparts, with female patients receiving one third less exposure.

Keywords: Coronary computed tomography angiography (CCTA); female; breast displacement; radiation exposure

Submitted Oct 26, 2014. Accepted for publication Dec 12, 2014.
doi: 10.3978/j.issn.2223-3652.2014.12.07
View this article at: http://dx.doi.org/10.3978/j.issn.2223-3652.2014.12.07

Introduction

Coronary computed tomography angiography (CCTA) has been described with continually decreasing radiation exposures, through various innovations (1-3). Radiation exposure in women is known to pose higher risks than in men and hence warrants increased caution (4). A primary driver of radiation risk to women undergoing CCTA is the highly radiosensitive female breasts, which are usually included in the z-axis range of scanning despite being a "non-target organ". The importance of radiation exposure to female patients is reflected in the International Commission of Radiation Protection

(ICRP)'s decision to increase the recommended breast tissue-weighting factor from 0.05 mSv/mGy/cm in 1990 to 0.12 mSv/mGy/cm in 2007.

Fortunately, the simple and low-cost intervention of displacing breasts out of the scan range has been reported (5,6). By displacing the mobile portion of the female breast out of the scan range, significantly reduced breast radiation dose has been demonstrated while improving or maintaining image quality compared to non-displacement of the breasts (6).

Previously, the use of automatic tube potential and tube current selection algorithms (APS-AEC) has been reported (6,7). The use of APS-AEC to set the indication-appropriate exposure settings based on the scout radiograph has been shown to reduce overall radiation exposure by 29.8% versus more traditional body mass index (BMI)-based methods of adjusting tube potential and tube current settings (7).

We sought to evaluate the combined effect of these two radiation lowering strategies (breast displacement in conjunction with AEC-APS) in women, who are the more radiation sensitive sex. Overall, we hypothesized that the combined use of APS-AEC with breast displacement in females would be associated with significant gender differences in CCTA radiation doses, with women benefitting from breast displacement out of the scan range. Thus we intended to evaluate if lower tube current and tube potential are selected if breasts are displaced. Because the primary goal of any diagnostic examination is to deliver accurate results, we also evaluated image quality.

Materials and methods

This study was approved by the human research committee of the institutional review board, and compliance with the Health Insurance Portability and Accountability Act guidelines was maintained. The authors maintained full control over the study design and data.

Patient population

The cohort of our retrospective study included 726 consecutive patients who underwent clinically indicated CCTA between January 2012 and July 2013. Only patients referred for native coronary scans were included, and patients who were referred for other indications such as coronary bypass graft evaluation, pulmonary vein mapping, congenital heart disease evaluation, aortic evaluation and research protocols were excluded. Patient parameters such as age, gender, BMI, weight, height, and heart rate during scan were collected from clinical records and CT reports. Male and female cohorts were stratified according to BMI ranges of <25, 25-29.9, 30-34.9 and >35 kg/m^2.

Scan protocol

All scans were performed using a second-generation dual-source scanner (SOMATOM Definition Flash; Siemens Healthcare, Forchheim, Germany; software update VA40). Per department protocol, one of three ECG synchronization modes were utilized; retrospectively ECG-gated helical, prospectively ECG-triggered axial-sequential (Adaptive Cardio Sequential, Siemens Healthcare), and prospectively ECG-triggered high-pitch helical scanning (HPH) (Flash Cardio, Siemens Healthcare), at the supervising physician's discretion when taking into account factors such as heart rate, heart rhythm, breath-hold capacity, and clinical information requested. Automatic tube potential selection software (APS-CARE kV; Siemens Healthcare) was used to select a tube potential from one of four values of 80, 100, 120, 140 kVp, based on the patient size as detected on the postero-anterior scout radiograph. In addition to APS, automatic tube current selection algorithm (AEC-CareDose 4D; Siemens Healthcare) was used in all cases. Calcium score was obtained in majority of the patients using prospective triggering acquisition technique with a constant tube potential of 120 kVp and mA tailored to the scout radiograph.

During the entire study period, female breast displacement was required as a matter of site policy for all cardiac CT exams at our site (*Figure 1A,B*). This was accomplished by using the Velcro patient positioning strap which is attached to the scanner table (Siemens Healthcare) and breasts in all female patients were displaced prior to acquisition of the scout images used for automatic tube potential and tube current selection.

Scans were performed during a single breath-hold at end inspiration, and the scan range covered from the level of the carina to the diaphragm. The test bolus method was used to correctly time the contrast agent administration to aortic peak enhancement plus 3-4 s delay. On average, a 60-80 mL bolus of iopamidol 370 g/cm^3 (Isovue 370; Bracco Diagnostics, Princeton, NJ, USA) was power-injected at a rate of 4.5 to 6 mL/s (based on patient size and intravenous access), followed by a 40 mL of saline flush at an identical rate. Depending on the nature of the case, beta-blockade (metoprolol tartrate 5 to 25 mg intravenously, in 5 mg

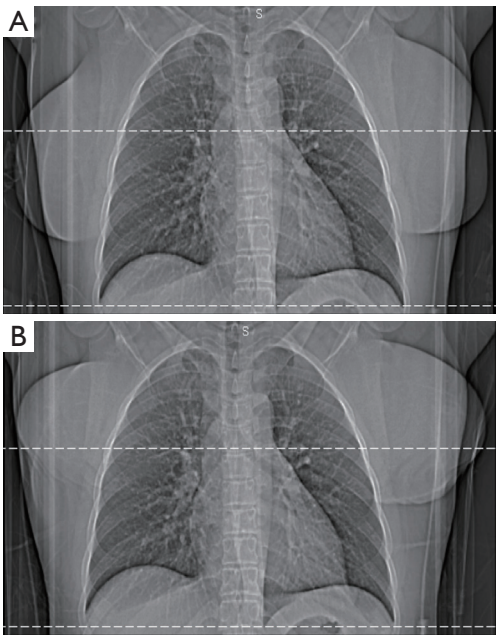

Figure 1 Pre breast displacement. (A) CCTA scout radiograph showing most part of mobile breast tissue lying in the z-axis of scan range; (B) post breast displacement. Breast displacement with patient positioning belt in place moves most part of mobile breast tissue out of the scan range. CCTA, coronary computed tomography angiography.

increments) was administered at the supervising physician's discretion. Unless contraindicated, sublingual nitroglycerine (0.6 mg tablet) was administered. Image reconstructions were used appropriate to coronary CTA were utilized (default 0.75 mm thick images at a 0.4 mm interval, using iterative reconstruction technique with a CTA-specific iterative reconstruction kernel "I31", Siemens Healthcare).

Data collection

Scan parameters including mode of ECG synchronization, median effective dose (ED), total and coronary acquisition dose length product (DLP), tube voltage (kV), tube current (mAs), CT dose index volume ($CTDI_{vol}$) were recorded. The scanner-generated dose exposure record and ECG tracing during scanning was archived, with which the actual dose parameters, heart rate, and rhythm were verified. Size specific dose estimate (SSDE) values were obtained for a subset of consecutive patients of the cohort (n=340) using dedicated software (Radimetrics Inc, Bayer AG, Toronto, Canada).

Image quality evaluation

We performed a quantitative image analysis using attenuation values of the lumen of the aorta, left main coronary artery and origin of the right coronary artery, as previously described (8). Briefly, we evaluated the proximal right coronary artery (RCA-American Heart Association classification segment #1) and left main (LM-American Heart Association classification segment #5) for each data set. Image quality was evaluated using OsiriX DICOM viewer (Pixmeo, Geneva, Switzerland). For each image analysis, background noise was determined by placing a region of interest (ROI) in the aortic root at a position cranial to the left coronary ostium and noting the standard deviation value in Hounsfield units. Attenuation within the lumens of proximal RCA and LM were calculated by placing the largest possible ROI within each lumen, and attenuation in the perivascular tissue was found by placing ROI next to either the proximal RCA or LM without including the vessel wall. Contrast-to-noise ratio (CNR) was calculated by dividing the difference in Hounsfield units between vessel (proximal RCA or LM) and perivascular fat by the uniform background noise. Signal-to-noise ratio (SNR) was determined by dividing attenuation values by image noise (9-12).

Statistical analysis

Continuous variables are expressed as mean ± SD or medians with interquartile range. Comparisons between groups were performed with the use of an independent sample *t*-test or Wilcoxon rank-sum test for continuous variables, Fisher's exact test for categorical variables, and the Wilcoxon rank-sum test for ordinal variables. A two-sided P value of less than 0.05 was considered to indicate statistical significance. For multivariable analyses, we employed three different median regression models with robust standard errors and ED, CTDI volume, or SSDE as dependent variables. In all models, female sex, age, BMI, average heart rate, HPH prospectively ECG-triggered mode, prospectively ECG-triggered axial-sequential mode and calcium score were used as independent variables. All statistical analyses were performed using Stata/SE 13.1 (StataCorp LP, College Station, Texas, USA).

Results

Patient characteristics and scan parameters

Patient clinical characteristics and scan parameters are

Table 1 Clinical characteristics and scan parameters of cohort stratified according to gender

Variables	Female (n=343)	Male (n=383)	P value
Age (years), mean ± SD	56.6±14.5	53.4±14.3	0.002
BMI, mean ± SD	28.6±6.9	29.2±6.3	0.168
BMI classification, n (%)			0.056
<25	124 (36.2)	84 (21.9)	
25-29.9	92 (26.8)	153 (40.0)	
30-34.9	65 (19.0)	93 (24.3)	
≥35	62 (18.1)	53 (13.8)	
Heart rate (beats/min), mean ± SD	64.6±10.9	64.0±12.0	0.479
Beta blockers, n (%)	227 (66.2)	236 (61.6)	0.216
Nitroglycerin, n (%)	311 (90.7)	348 (90.9)	1.000
Total tube current (mAs), median [IQR]	1,844 [1,453-2,538]	2,120 [1,701-2,722]	<0.001
Cardiac tube current (mAs), median [IQR]	243 [178-316]	257 [203-334]	0.003
Tube potential (kV), n (%)			<0.001
80	132 (38.5)	61 (15.9)	
100	121 (35.3)	175 (45.7)	
120	74 (21.6)	121 (31.6)	
140	16 (4.7)	26 (6.8)	
Scanner mode, n (%)			
Retrospective ECG-gating	48 (14.3)	43 (11.5)	0.268
Prospective triggering	261 (76.1)	293 (76.5)	0.930
High pitch helical acquisition	34 (9.9)	47 (12.3)	0.346
Calcium scoring, n (%)	222 (64.7)	262 (68.4)	0.306

SD, standard deviation; BMI, body mass index (kg/m^2).

shown in *Table 1* and detailed result according to BMI ranges is shown in *Table S1*. Out of our total cohort of 726 patients, 343 (47%) were female. On an average, females were older than males (56.6 *vs.* 53.4, P=0.002). The average BMI in females was 28.6 and 29.2 kg/m^2 in males, the difference not being significant (P=0.168). Scans were completed using retrospectively ECG-gated (12.5%, n=91), prospectively ECG-triggered (76.3%, n=554) and prospective ECG-triggered high pitch helical mode (11.1%, n=81). Of prospectively ECG-triggered scans, 186 scans (33.5%) and 368 scans (66.4%) were acquired during a fixed range of systole as described previously, or diastole, respectively (13). Calcium score was obtained in a similar proportion of both the groups 65% of females (n=222) and in 68% of males (n=262).

Univariable analysis

Comparison of the unadjusted radiation dose between males and females was performed using ED, $CTDI_{vol}$ and SSDE as shown in *Tables 2,3*. The overall ED was 1.3 mSv (i.e., –32.3%) lower in females than in males (P<0.001). The difference in ED was highly significant in all BMI groups (P<0.001) except BMI ≥35 (P=0.149) as shown in *Figure 2A*. Median $CTDI_{vol}$ was 8.6 *vs.* 12.7 mGy for females and males respectively (P<0.001). For females, $CTDI_{vol}$ was lower in patients with BMI <30 kg/m^2 (P≤0.035). However no significant difference was found in patients with BMI ≥30 kg/m^2 (*Figure 2B*). In a subset analysis by SSDE, females had 6.8 mGy lower median SSDE than males (P<0.001) (i.e., –34.2%). Among the various BMI groups, only the group with BMI 25-29.9 showed a statistically difference in median SSDEs between females and males (P<0.001) (*Figure 2C*). The *Tables 4-9* demonstrate radiation dose differences based on different CCTA acquisition modes. While there were significant differences in the radiation dose for the prospective triggering method, there were no statistically significant differences for the retrospective ECG-gating and the high pitch helical acquisition gating methods (which are most likely due to the small number of patients, on the basis of their infrequent use).

Multivariable analysis

Results of the multivariable median regression analyses are shown in *Table 10*. After controlling for age, BMI, mean heart rate, acquisition mode, and calcium score, the median ED was 0.7 mSv lower for females (P<0.001). We found similar results for CTD_{Ivol} and SSDE with median differences of –2.3 and –3.15 mGy, respectively (P<0.001).

Image quality analysis

Overall, both male and female patients' image quality was similar (*Table 11*). Aortic noise, RCA attenuation, RCA CNR, RCA SNR, LM attenuation, LM CNR, and SNR values are shown in *Table 4*. Both male and female patients'

Table 2 Radiation exposure stratified according to gender and BMI

Variables	Female (n=343)	Male (n=383)	P value
Effective dose (mSv), median (IQR)			
Overall	2.3 (1.4-5.2)	3.6 (2.5-5.9)	<0.001
BMI <25	1.4 (1.2-2.2)	2.1 (1.4-3.2)	<0.001
BMI 25-29.9	2.0 (1.4-3.2)	3.2 (2.4-4.3)	<0.001
BMI 30-34.9	3.1 (2.3-5.8)	4.4 (3.4-7.0)	<0.001
BMI ≥35	7.2 (4.9-9.1)	7.7 (6.0-11.3)	0.149
$CTDI_{vol}$ (mGy), median (IQR)			
Overall	8.6 (4.9-20.0)	12.7 (7.3-22.7)	<0.001
BMI <25	4.9 (3.8-7.7)	6.4 (4.3-10.1)	0.035
BMI 25-29.9	6.7 (5.0-12.7)	11.5 (7.7-15.3)	<0.001
BMI 30-34.9	13.3 (8.5-24.6)	17.3 (11.8-25.0)	0.106
BMI ≥35	26.6 (17.4-35.5)	28.9 (23.2-37.8)	0.196

BMI, body mass index (kg/m^2); IQR, interquartile range; $CTDI_{vol}$, CT dose index volume.

Table 3 Radiation exposure stratified according to gender and BMI

SSDE (mGy), median (IQR)	Female (n=159)	Male (n=181)	P value
Overall	13.1 (8.2-28.2)	19.9 (12.0-30.3)	<0.001
BMI <25	8.5 (6.7-13.8)	10.9 (8.3-16.7)	0.086
BMI 25-29.9	11.5 (8.3-16.1)	16.7 (12.8-24.0)	<0.001
BMI 30-34.9	26.8 (12.3-45.8)	29.8 (19.6-37.2)	0.371
BMI ≥35	39.2 (23.6-51.7)	33.4 (27.0-54.3)	0.884

BMI, body mass index (kg/m^2); SSDE, size specific dose estimate; IQR, interquartile range.

Table 4 Radiation exposure stratified according to gender and BMI-retrospective ECG-gating only

Variables	Female (n=48)	Male (n=43)	P value
Effective dose (mSv), median (IQR)			
Overall	5.9 (3.3-9.4)	7.0 (4.7-13.0)	0.063
BMI <25	3.6 (2.7-6.9)	4.9 (2.5-11.5)	0.626
BMI 25-29.9	6.5 (4.3-6.9)	5.4 (3.8-6.9)	0.835
BMI 30-34.9	5.9 (4.4-10.4)	8.3 (5.9-13.8)	0.166
BMI ≥35	13.5 (9.0-14.0)	12.3 (11.0-14.5)	0.745
$CTDI_{vol}$ (mGy), median (IQR)			
Overall	20.3 (9.9-36.5)	21.6 (12.3-48.0)	0.309
BMI <25	12.4 (8.7-20.6)	11.0 (8.1-27.9)	0.922
BMI 25-29.9	20.0 (9.0-30.8)	14.8 (10.9-20.6)	0.493
BMI 30-34.9	25.1 (16.5-47.1)	39.5 (21.6-58.2)	0.356
BMI ≥35	43.1 (32.8-50.7)	47.5 (31.1-50.1)	0.914

BMI, body mass index (kg/m^2); IQR, interquartile range; $CTDI_{vol}$, CT dose index volume.

Table 5 Radiation exposure stratified according to gender and BMI-retrospective ECG-gating only

SSDE (mGy), median (IQR)	Female (n=31)	Male (n=27)	P value
Overall	26.9 (14.7-50.9)	28.3 (20.4-54.5)	0.450
BMI <25	17.2 (12.7-28.5)	20.4 (9.7-23.5)	0.881
BMI 25-29.9	22.6 (16.4-23.8)	27.6 (20.4-28.3)	0.195
BMI 30-34.9	50.9 (46.6-64.3)	42.4 (36.6-47.2)	0.223
BMI ≥35	56.2 (40.9-74.5)	50.1 (30.7-61.0)	0.286

BMI, body mass index (kg/m^2); SSDE, size specific dose estimate; IQR, interquartile range.

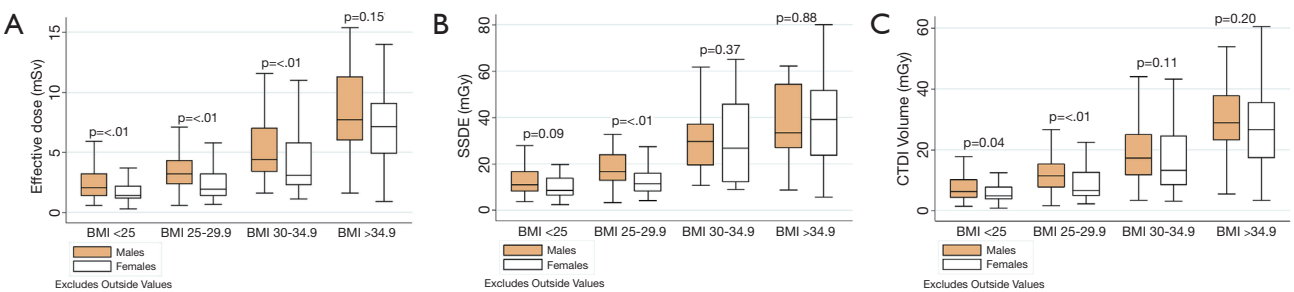

Figure 2 A box plot showing radiation exposure by gender and BMI groups. (A) Effective dose; (B) $CTDI_{vol}$; (C) SSDE. BMI, body mass index; $CTDI_{vol}$, CT dose index volume; SSDE, size-specific dose estimate.

Table 6 Radiation exposure stratified according to gender and BMI-prospective triggering only

Variables	Female (n=261)	Male (n=293)	P value
Effective dose (mSv), median (IQR)			
Overall	2.1 (1.3-4.3)	3.5 (2.4-5.2)	<0.001
BMI <25	1.3 (1.0-1.8)	2.0 (1.4-2.8)	<0.001
BMI 25-29.9	1.9 (1.5-2.8)	3.0 (2.4-3.9)	<0.001
BMI 30-34.9	2.7 (2.0-4.6)	4.2 (3.4-6.0)	<0.001
BMI ≥35	6.6 (4.4-9.0)	7.2 (6.0-9.4)	0.181
$CTDI_{vol}$ (mGy), median (IQR)			
Overall	8.2 (4.9-17.5)	12.9 (8.4-21.7)	<0.001
BMI <25	4.5 (3.8-6.5)	6.5 (4.6-10.1)	<0.001
BMI 25-29.9	6.9 (5.4-12.4)	11.6 (8.9-15.2)	<0.001
BMI 30-34.9	12.9 (7.8-23.5)	17.4 (12.4-23.3)	0.012
BMI ≥35	26.0 (17.5-32.2)	27.0 (23.2-32.3)	0.339

BMI, body mass index (kg/m^2); IQR, interquartile range; $CTDI_{vol}$, CT dose index volume.

Table 7 Radiation exposure stratified according to gender and BMI-prospective triggering only

SSDE (mGy), median (IQR)	Female (n=116)	Male (n=141)	P value
Overall	11.6 (7.8-23.5)	19.3 (11.9-27.7)	<0.001
BMI <25	7.8 (6.4-10.8)	10.9 (9.0-14.4)	0.003
BMI 25-29.9	10.8 (8.5-14.9)	16.6 (13.2-22.1)	<0.001
BMI 30-34.9	19.2 (11.4-31.6)	26.4 (19.3-35.2)	0.110
BMI ≥35	37.3 (20.9-48.7)	31.7 (24.8-49.5)	0.989

BMI, body mass index (kg/m^2); SSDE, size specific dose estimate; IQR, interquartile range.

Table 8 Radiation exposure stratified according to gender and BMI-high pitch helical acquisition only

Variables	Female (n=34)	Male (n=47)	P value
Effective dose (mSv), median (IQR)			
Overall	1.9 (1.2-3.4)	3.0 (1.5-4.9)	0.063
BMI <25	1.4 (1.0-2.0)	1.2 (0.9-2.7)	0.931
BMI 25-29.9	1.6 (1.0-3.0)	3.6 (1.6-5.4)	0.034
BMI 30-34.9	2.9 (2.4-4.7)	4.0 (3.0-7.0)	0.165
BMI ≥35	7.3 (5.4-9.1)	5.1 (4.8-5.3)	0.083
$CTDI_{vol}$ (mGy), median (IQR)			
Overall	4.5 (2.6-6.3)	5.7 (2.8-10.2)	0.174
BMI <25	2.5 (1.5-4.9)	2.4 (2.2-3.0)	0.977
BMI 25-29.9	4.1 (2.7-5.5)	5.7 (3.1-13.6)	0.161
BMI 30-34.9	9.2 (5.9-15.5)	7.3 (6.9-10.1)	0.758
BMI ≥35	9.3 (6.5-15.7)	8.8 (7.4-10.1)	1.000

IQR, interquartile range; BMI, body mass index (kg/m^2); $CTDI_{vol}$, CT dose index volume.

Table 9 Radiation exposure stratified according to gender and BMI-high pitch helical acquisition only

SSDE (mGy), median (IQR)	Female (n=12)	Male (n=13)	P value
Overall	8.2 (5.6-17.9)	11.4 (6.7-17.8)	0.664
BMI <25	7.0 (4.8-8.2)	5.4 (3.7-6.7)	0.480
BMI 25-29.9	6.2 (4.8-9.1)	11.4 (7.1-14.0)	0.186
BMI 30-34.9	26.3 (9.0-27.7)	31.2 (17.8-44.6)	0.564
BMI ≥35*	24.7 (–)	18.0 (–)	–

*, only 1 patient per category. BMI, body mass index (kg/m^2); SSDE, size specific dose estimate; IQR, interquartile range.

proximal RCA and LM CNR values (14.6±4.1 *vs.*15.8±4.3 and 15.3±3.3 *vs.* 15.9±4.3, respectively) are shown to be greater than 11.4±4.2, indicating superior image quality (8). A significant difference was observed between male and female patients regarding the CNR of only the proximal RCA (P<0.05).

Discussion

We found a significant gender difference in radiation exposure of CCTA with the combined use of an APS-AEC protocol and breast displacement out of the scan range in females, with females receiving less radiation exposure than protocol matched males across all BMI ranges. Image quality of scans was maintained at excellent objective diagnostic quality (CNR >11.4±4.2) for coronary artery evaluation. To our knowledge, no studies have evaluated the combined effects of modulation of the X-ray tube potential and tissue manipulation in the scanned range of CCTA to achieve reasonably lower exposure. Also, our prescription of CT acquisitions was based on clinical indication for coronary artery evaluation and individual patient characteristics. Our patient specific protocols optimized image quality for evaluation of coronary artery

Table 10 Multivariable median regression analysis*

Independent variables	Model 1 (effective dose)		Model 2 ($CTDI_{vol}$)		Model 3 (SSDE)	
	Coeff. (95% CI)	P value	Coeff. (95% CI)	P value	Coeff. (95% CI)	P value
Female	–0.68 (–0.92, –0.43)	<0.001	–2.30 (–3.34, –1.26)	<0.001	–1.91 (–3.56, –0.26)	0.024
Age	0.02 (0.01, 0.02)	<0.001	0.05 (0.01, 0.08)	0.003	0.06 (0.01, 0.10)	0.016
BMI	0.26 (0.23, 0.29)	<0.001	1.00 (0.89, 1.11)	<0.001	1.38 (1.18, 1.58)	<0.001
Mean Heart Rate	0.03 (0.01, 0.04)	<0.001	0.13 (0.08, 0.18)	<0.001	0.08 (0.00, 0.15)	0.047
HPH (flash mode)	–2.86 (–3.78, –1.93)	<0.001	–12.86 (–16.18, –9.54)	<0.001	–18.57 (–22.57, –14.57)	<0.001
Prospective triggering	–2.87 (–3.68, –2.07)	<0.001	–8.35 (–11.38, –5.33)	<0.001	–11.45 (–14.75, –8.16)	<0.001
Ca score	0.41 (0.18, 0.65)	<0.001	–0.21 (–1.3, 0.97)	0.726	–6.41 (–8.57, –4.25)	<0.001
Observations	720	–	720	–	337	–
Pseudo R-squared	0.34	–	0.32	–	0.31	–

*using robust standard errors. $CTDI_{vol}$, CT dose index volume; SSDE, size-specific dose estimate; BMI, body mass index; HPH, prospective triggered high pitch helical scanning mode.

Table 11 Image quality analysis within prospectively-ECG triggered scans in a consistently fixed range of late systole to early diastole

Variables	Female (n=88)	Male (n=98)	P value
Aorta noise (HU), mean ± SD	36.9±10.8	31.5±9.5	<0.001
RCA signal (HU) , mean ± SD	446.5±123.3	397.4±120.2	0.007
RCA CNR, mean ± SD	14.6±4.1	15.8±4.3	0.04
RCA SNR, mean ± SD	12.1±3.3	13.0±3.3	0.07
LM signal (HU), mean ± SD	472.4±128.8	413.2±118.6	0.001
LM CNR, mean ± SD	15.3±3.3	15.9±4.3	0.26
LM SNR, mean ± SD	13.2±3.14	13.6±3.3	0.43

RCA, right coronary artery; SD, standard deviation; CNR, contrast-to-noise ratio; SNR, signal-to-noise ratio; LM: left main coronary artery.

disease, to a reasonable limit while preserving image quality, thus often favoring acquisition of several phases (prospective triggering), rather than the absolute limit of dose by using HPH prospective ECG-triggered mode (14).

Our findings are in agreement with and incremental to those from prior studies of breast displacement (6,15). A prior study showed that lowering of tube voltages improved contrast medium and skeletal imaging (without affecting the CNR) and significantly reduced radiation exposure to female breast tissue (15). We previously observed that appropriate selection of tube potential via automated tube voltage and current modulation significantly reduced overall radiation exposure to most patients undergoing CCTA. Notably, images of both our male and female cohort were again maintained at a superior quality (7). Previously, the use of thermoluminescent dosimetry (TLD) badges to evaluate the direct exposure to breast tissue has established that breast displacement out of the scan range reduced mean breast surface dose by 23% (6). Thus, in conjunction with the prior work in this area, our work further justifies the use of breast displacement in female patients undergoing CCTA when possible and is in accordance with the (as low as reasonably achievable) ALARA principle.

Einstein *et al.* calculated risk of radiation exposure from CCTA and observed that the lifetime cancer risk estimates for standard cardiac scans varied from 1 in 143 for a 20-year-old woman to 1 in 3,261 for an 80-year-old man. The most affected organs were lungs and breasts receiving 42-91 and 40-80 mSv radiation dose respectively and the highest organ lifetime attributable risk (LAR) were for lung cancer and, in younger women, breast cancer. The LAR for female was greater than that for male at all ages, with the relative risk of female ranging from 2.4 at age 80 years to 4.8 at age 20 years. Thus Einstein et al. concluded that the breast cancer risk was considerably higher in younger female patients (16).

Because breast tissues have a relatively high tissue-weighting factor, various approaches of reducing dose to the female breast in thoracic CT have been investigated

(17-19). Our method confers an overall dose advantage in women, and also prevents the exposure to relatively higher-risk breast tissue. Thus, the average exposure to breast tissue itself will be further lowered using this method. In fact, this may lead to a slight overestimation of the radiation risk to women at CCTA on a population basis (when using traditionally published weighting factors), when using breast displacement techniques. This is because displaced female breasts receive less radiation exposure, on the basis of avoiding direct X-ray irradiation, and by lowering the necessary overall dose necessary to achieve diagnostic CCTA.

Prior studies have established the efficacy of using simple measurements like BMI to stratify and adjust radiation exposure settings for cardiac CT imaging, but the use of patients' actual chest measurements in the region of scanning are clearly more desirable (20,21). Additionally, there are known gender differences in adiposity of men and women, particularly in regard to the proportion of android (upper body) and gynecoid (lower body) regions of tissue composition, further supporting the need for tailored dose parameters in women versus men (22). This is compounded by the development of SSDE, which is thought to better estimate an actual patients' risk due to radiation exposure on the basis of body size versus $CTDI_{vol}$ (23). Although SSDE is presumably accurate to within 10-20%, we chose to incorporate both $CTDI_{vol}$ and SSDE to mitigate any possible biases or limitations in either method (24,25).

Our breast displacement technique has certain advantages over the use of breast shields. Quantitative study for assessment of selective organ shielding with lead- or bismuth containing protective materials have been done by Geleijns *et al*. Studies performed with phantoms and patients suggest that shielding results in an increase of image noise and results in only modest reductions of radiation exposure (26). In contrast, our method demonstrates superior image quality with CNR greater than 11.4±4.2 in proximal RCA and LM.

Our methods bear some limitations. Most notably, our design lacked a control group for non AEC-APS and non-displaced breast tissue patients. Since our site practice has been to displace breasts for the past several years on the basis of robust prior studies, we felt it would be unethical to expose women's breast tissue to radiation solely to establish a control group. In addition, SSDE values were derived directly from a relatively new software (Radimetrics Inc., Bayer AG, Toronto, Canada) which uses a "center slice" technique that may not account for the "hourglass" shape of the female figure. Further, we have not taken into account different breast cup sizes in our study, as it was done in a previous study (6) since these were not recorded in our retrospective cohort. The use of varied CCTA gating methods subdivided our cohort, and this choice is difficult to control, as gating methodologies depend heavily on patient factors at the time of scanning, and the supervising physician's discretion. Finally, we also utilized only the scanner-generated exposure metrics ($CTDI_{vol}$ and DLP) to calculate ED (27). While $CTDI_{vol}$ and DLP have limitations in that they are independent of patient size, patient dose is not actually independent of size (23). Furthermore, $CTDI_{vol}$ and DLP may be displayed for either a 16- or 32-cm diameter reference phantom. If the 32-cm phantom is referenced for smaller patients, interpretation of $CTDI_{vol}$ or DLP as a patient dose without a size correction is known to underestimate dose by a factor of 2-3 (23). Again noted are the gender differences in body size (i.e., differences in fat and muscle mass) which may affect BMI and radiation dose. We have mitigated the difference by utilizing SSDE which specifically and accurately measures the radiation dose based on effective diameter. We also did not directly measure breast tissue exposures, as opposed to the work of Foley *et al.* (6); we presume that in addition to the more pronounced overall radiation savings the current protocol achieved, a similar effect would be noted on breast tissue, and in turn the implicit stochastic cancer risks associated with this scan protocol. As a future implication, this method would further reduce radiation dose in females and could be used for obese male patients with large breasts as a means for reducing radiation exposure to breast tissue.

Conclusions

We observed a difference in radiation exposure to patients undergoing CCTA with the combined use of AEC-APS and breast displacement in female patients as compared to their BMI-matched male counterparts, with female patients receiving one third less exposure. This has important clinical implications for female patients, as their breasts have a high tissue-weighting factor. We also report a possible application of SSDE to more critically study CCTA radiation exposure.

Acknowledgements

Authors' contribution: Harshna Vadvala: data collection,

manuscript writing; Phillip Kim: data collection; Thomas Mayrhofer: statistical analysis; Oleg Pianykh: statistical data contribution; Mannudeep Kalra: concept and manuscript editing; Udo Hoffmann: concept and manuscript editing; Brian Ghoshhajra: concept, manuscript editing and project supervision.

Disclosure: The authors declare no conflict of interest.

References

1. Ghoshhajra BB, Engel LC, Major GP, et al. Evolution of coronary computed tomography radiation dose reduction at a tertiary referral center. Am J Med 2012;125:764-72.
2. Bischoff B, Hein F, Meyer T, et al. Impact of a reduced tube voltage on CT angiography and radiation dose: results of the PROTECTION I study. JACC Cardiovasc Imaging 2009;2:940-6.
3. Chinnaiyan KM, Boura JA, DePetris A, et al. Progressive radiation dose reduction from coronary computed tomography angiography in a statewide collaborative quality improvement program: results from the Advanced Cardiovascular Imaging Consortium. Circ Cardiovasc Imaging 2013;6:646-54.
4. Goodman TR, Amurao M. Medical imaging radiation safety for the female patient: rationale and implementation. Radiographics 2012;32:1829-37.
5. Paul JF, Abada HT. Strategies for reduction of radiation dose in cardiac multislice CT. Eur Radiol 2007;17:2028-37.
6. Foley SJ, McEntee MF, Achenbach S, et al. Breast surface radiation dose during coronary CT angiography: reduction by breast displacement and lead shielding. AJR Am J Roentgenol 2011;197:367-73.
7. Ghoshhajra BB, Engel LC, Károlyi M, et al. Cardiac computed tomography angiography with automatic tube potential selection: effects on radiation dose and image quality. J Thorac Imaging 2013;28:40-8.
8. Ferencik M, Nomura CH, Maurovich-Horvat P, et al. Quantitative parameters of image quality in 64-slice computed tomography angiography of the coronary arteries. Eur J Radiol 2006;57:373-9.
9. Hausleiter J, Meyer TS, Martuscelli E, et al. Image quality and radiation exposure with prospectively ECG-triggered axial scanning for coronary CT angiography: the multicenter, multivendor, randomized PROTECTION-III study. JACC Cardiovasc Imaging 2012;5:484-93.
10. Feuchtner GM, Jodocy D, Klauser A, et al. Radiation dose reduction by using 100-kV tube voltage in cardiac 64-slice computed tomography: a comparative study. Eur J Radiol 2010;75:e51-6.
11. Bittencourt MS, Schmidt B, Seltmann M, et al. Iterative reconstruction in image space (IRIS) in cardiac computed tomography: initial experience. Int J Cardiovasc Imaging 2011;27:1081-7.
12. Wang D, Hu XH, Zhang SZ, et al. Image quality and dose performance of 80 kV low dose scan protocol in high-pitch spiral coronary CT angiography: feasibility study. Int J Cardiovasc Imaging 2012;28:415-23.
13. Lee AM, Beaudoin J, Engel LC, et al. Assessment of image quality and radiation dose of prospectively ECG-triggered adaptive dual-source coronary computed tomography angiography (cCTA) with arrhythmia rejection algorithm in systole versus diastole: a retrospective cohort study. Int J Cardiovasc Imaging 2013;29:1361-70.
14. Schoenhagen P, Baker ME. Our preoccupation with ultra-low dose radiation exposure. Low contrast resolution and cardiovascular CT imaging. J Cardiovasc Comput Tomogr 2014;8:426-8.
15. Vollmar SV, Kalender WA. Reduction of dose to the female breast as a result of spectral optimisation for high-contrast thoracic CT imaging: a phantom study. Br J Radiol 2009;82:920-9.
16. Einstein AJ, Henzlova MJ, Rajagopalan S. Estimating risk of cancer associated with radiation exposure from 64-slice computed tomography coronary angiography. JAMA 2007;298:317-23.
17. Yilmaz MH, Albayram S, Yaşar D, et al. Female breast radiation exposure during thorax multidetector computed tomography and the effectiveness of bismuth breast shield to reduce breast radiation dose. J Comput Assist Tomogr 2007;31:138-42.
18. Hohl C, Wildberger JE, Süss C, et al. Radiation dose reduction to breast and thyroid during MDCT: effectiveness of an in-plane bismuth shield. Acta Radiol 2006;47:562-7.
19. Geleijns J, Salvadó Artells M, Veldkamp WJ, et al. Quantitative assessment of selective in-plane shielding of tissues in computed tomography through evaluation of absorbed dose and image quality. Eur Radiol 2006;16:2334-40.
20. Husmann L, Herzog BA, Burkhard N, et al. Low-dose coronary CT angiography with prospective ECG triggering: validation of a contrast material protocol adapted to body mass index. AJR Am J Roentgenol 2009;193:802-6.
21. Ghoshhajra BB, Engel LC, Major GP, et al. Direct chest area measurement: A potential anthropometric replacement for BMI to inform cardiac CT dose

parameters? J Cardiovasc Comput Tomogr 2011;5:240-6.
22. Ley CJ, Lees B, Stevenson JC. Sex- and menopause-associated changes in body-fat distribution. Am J Clin Nutr 1992;55:950-4.
23. Brady SL, Kaufman RA. Investigation of American Association of Physicists in Medicine Report 204 size-specific dose estimates for pediatric CT implementation. Radiology 2012;265:832-40.
24. Strauss KJ, Goske MJ. Estimated pediatric radiation dose during CT. Pediatr Radiol 2011;41:472-82.
25. Seibert JA, Boone JM, Wootton-Gorges SL, et al. Dose is not always what it seems: where very misleading values can result from volume CT dose index and dose length product. J Am Coll Radiol 2014;11:233-7.
26. Geleijns J, Salvadó Artells M, Veldkamp WJ, et al. Quantitative assessment of selective in-plane shielding of tissues in computed tomography through evaluation of absorbed dose and image quality. Eur Radiol 2006;16:2334-40.
27. Gerber TC, Kuzo RS, Morin RL. Techniques and parameters for estimating radiation exposure and dose in cardiac computed tomography. Int J Cardiovasc Imaging 2005;21:165-76.

Cite this article as: Vadvala H, Kim P, Mayrhofer T, Pianykh O, Kalra M, Hoffmann U, Ghoshhajra B. Coronary CTA using scout-based automated tube potential and current selection algorithm, with breast displacement results in lower radiation exposure in females compared to males. Cardiovasc Diagn Ther 2014;4(6):470-479. doi: 10.3978/j.issn.2223-3652.2014.12.07

Table S1 Patient characteristics and scan parameters in both gender stratified according to BMI classes

Variables	Overall (N=726)	BMI (male, N=383)				BMI (female, N=343)			
		<25 (N=84)	25-29.9 (N=153)	30-34.9 (N=93)	≥35 (N=53)	<25 (N=124)	25-29.9 (N=92)	30-34.9 (N=65)	≥35 (N=62)
Age, mean ± SD, year	54.9±14.5	54.6±17.2	53.9±13.9	53.4±12.5	49.7±13.2	54.8±16.4	58.2±13.7	57.6±13.8	57.1±11.8
Heart rate, mean ± SD, beats/min	64.9±11.9	61.2±13.1	63.4±10.8	65.0±10.9	68.4±14.3	63.3±10.2	64.6±10.8	67.1±13.0	64.8±10.0
Total tube current, mean ± SD, mAs	2,417.3±1,560.8	2,200.2±1,238.5	2,303.0±1,275.0	2,732.3±2,280.7	3,401.0±1,505.4	2,118.9±1,740.6	1,974.7±1,070.3	2,329.0±1,081.2	3,034.0±1,451.1
Cardiac tube current, mean ± SD, mAs	347.0±631.4	301.6±393.0	325.6±447.7	314.1±322.7	504.8±808.3	338.4±1047.3	264.7±227.6	299.3±234.0	569.3±943.5
Tube potential									
80 kV, n (%)	193 (26.5)	44 (52.4)	15 (9.7)	1 (1.1)	1 (1.9)	84 (67.7)	36 (39.1)	10 (15.4)	2 (3.2)
Retrospective-gating	17	3	1	0	0	10	2	1	0
Prospective-triggering	164	39	13	1	1	68	31	9	2
High-pitch helical acquisition	12	2	1	0	0	6	3	0	0
100 kV, n (%)	296 (40.8)	31 (36.9)	102 (66.7)	39 (41.9)	3 (5.7)	31 (25.0)	39 (42.4)	34 (52.3)	17 (27.4)
Retrospective-gating	38	3	13	3	0	10	4	5	0
Prospective-triggering	221	19	76	35	3	18	27	27	17
High-pitch helical acquisition	39	9	15	1	0	4	8	2	0
120 kV, n (%)	195 (26.8)	9 (10.7)	33 (21.3)	37 (39.8)	42 (79.2)	7 (5.7)	17 (18.5)	15 (23.1)	35 (56.5)
Retrospective-gating	33	2	2	5	9	2	3	5	5
Prospective-triggering	137	6	24	26	32	3	10	8	28
High-pitch helical acquisition	25	1	7	6	1	2	4	2	2
140 kV, n (%)	42 (5.8)	0	3 (1.9)	16 (17.2)	7 (13.2)	2 (1.6)	0	6 (9.2)	8 (12.9)
Retrospective-gating	5	0	0	2	1	0	0	1	1
Prospective-triggering	32	0	2	12	5	2	0	5	6
High-pitch helical acquisition	5	0	1	2	1	0	0	0	1
Beta blockers, n (%)	463 (63.8)	52 (61.9)	90 (58.8)	57 (61.3)	37 (69.8	76 (61.3)	62 (67.4)	46 (70.8)	43 (69.4)
Nitrogelycerin, n (%)	659 (90.8)	75 (89.3)	136 (88.9)	86 (92.4)	51 (96.2	114 (91.9)	82 (89.1)	61 (93.8)	54 (87.1)
Calcium scoring, n (%)	484 (66.7)	51 (60.7)	108 (70.6)	67 (72.0)	38 (71.7	86 (69.4)	61 (66.3)	36 (55.4)	39 (62.9)
Retrospective gating, n	93	8	16	10	10	22	9	12	6
Prospective triggering, n	554	64	114	74	41	91	68	49	53
High-pitch helical acquisition, n	81	12	24	9	2	12	15	4	3
$CTDI_{vol}$, median (IQR), mGy									
Retrospective-gating	20.6 (10.3-42.2)	11.0 (8.1-27.9)	14.7 (9.1-20.6)	39.5 (21.6-58.2)	47.5 (31.1-50.1)	11.4 (8.7-20.6)	20.0 (9.0-30.8)	25.1 (16.52-47.1)	43.1 (32.8-50.7)
Prospective-triggering	11.1 (6.2-20.5)	6.5 (4.6-10.1)	11.6 (8.9-15.2)	17.4 (12.4-23.3)	27.3 (23.4-32.8)	4.5 (3.8-6.5)	6.9 (5.4-12.4)	12.9 (7.8-23.5)	26.0 (17.5-32.2)
High-pitch helical acquisition	4.9 (2.6-7.4)	2.4 (2.2-3.0)	5.7 (3.1-13.6)	7.3 (6.9-10.1)	8.8 (7.4-10.2)	2.5 (1.5-4.9)	4.1 (2.7-5.5)	9.2 (5.9-15.5)	9.3 (6.5-15.7)
Coronary DLP, median (IQR), mGy·cm	154.0 (84.0-302.0)	96.0 (64.0-162.0)	161.0 (112.0-218.0)	239.0 (169.0-379.0)	391.0 (320.0-584.0)	71.0 (51.5-110.0)	100.0 (72.5-176.0)	171.0 (108.0-341.0)	355.0 (211.0-445.0)
Total DLP, median (IQR), mGy·cm	226.50 (129.0-417.0)	159.0 (103.5-251.0)	231.0 (175.0-319.0)	326.0 (247.0-506.0)	575.0 (429.0-842.0)	104.5 (85.0-163.0)	140.5 (103.0-240.5)	230.0 (163.0-442.0)	515.5 (350.0-660.0)

BMI, body mass index; $CTDI_{vol}$, CT dose index volume; IQR, interquartile range; DLP, dose length product.